

Zero-Shot Low-Light Image Enhancement via RGB–NIR Implicit Fusion

By

HIRAKJYOTI MEDHI

Admission No: 23MS0063



Submitted to:

**INDIAN INSTITUTE OF TECHNOLOGY
(INDIAN SCHOOL OF MINES), DHANBAD**

For the award of the degree of
MASTER OF SCIENCE

MAY, 2025



**INDIAN INSTITUTE OF TECHNOLOGY
(INDIAN SCHOOL OF MINES)
DHANBAD**

**CERTIFICATE FOR THE FINAL VERSION OF
DISSERTATION**

(To be submitted at the time of Final Dissertation Submission)

This is to certify that the Dissertation entitled “**Zero-Shot Low-Light Image Enhancement via RGB–NIR Implicit Fusion**” being submitted to the Indian Institute of Technology (Indian School of Mines), Dhanbad, by **Mr. Hirakjyoti Medhi**, **Admission No: 23MS0063** for the award of the Degree of **Master Of Science** from IIT (ISM), Dhanbad, is a bonafide work carried out by him, in the Department of **Mathematics and Computing**, IIT (ISM), Dhanbad, under my supervision and guidance. The dissertation has fulfilled all the requirements as per the regulations of this Institute and, in my opinion, has reached the standard needed for submission. The results embodied in this dissertation have not been submitted to any other university or institute for the award of any degree or diploma.

Signature of Supervisor (s)

Name: Prof. Sudhakar Kumawat

Date:



**INDIAN INSTITUTE OF TECHNOLOGY
(INDIAN SCHOOL OF MINES)
DHANBAD**

DECLARATION BY THE STUDENT

(To be submitted at the time of Final Dissertation Submission)

I hereby declare that the work which is being presented in this dissertation entitled “**Zero-Shot Low-Light Image Enhancement via RGB–NIR Implicit Fusion**” in partial fulfillment of the requirements for the award of the degree of Master of Science in **Mathematics and Computing** is an authentic record of my own work carried out during the period from **January 2025 to April 2025** under the supervision of **Asst. Prof. Sudhakar Kumawat**, Department of **Mathematics and Computing**, Indian Institute of Technology (ISM), Dhanbad, Jharkhand, India.

I acknowledge that I have read and understood the UGC (Promotion of Academic Integrity and Prevention of Plagiarism in Higher Educational Institutions) Regulations, 2018. These Regulations were published in the Indian Official Gazette on 31st July, 2018.

I confirm that this Dissertation has been checked for plagiarism using the online plagiarism checking software provided by the Institute. At the end of the Dissertation, a copy of the summary report demonstrating similarities in content and its potential source (if any), generated online using plagiarism checking software, is enclosed. I hereby confirm that the Dissertation has less than 10% similarity according to the plagiarism checking software’s report and meets the MoE/UGC Regulations as well as the Institute’s rules for plagiarism.

I further declare that no portion of the dissertation or its data will be published without the Institute’s or Guide’s permission. I have not previously applied for any other degree or award using the topics and findings described in my dissertation.

Hirakjyoti Medhi

Admission No.: 23MS0063

Department of Mathematics & Computing

IIT (ISM), Dhanbad



INDIAN INSTITUTE OF TECHNOLOGY
(INDIAN SCHOOL OF MINES)
DHANBAD

CERTIFICATE FOR CLASSIFIED DATA

(To be submitted at the time of Final Dissertation Submission)

This is to certify that the Dissertation entitled “**Zero-Shot Low-Light Image Enhancement via RGB–NIR Implicit Fusion**” being submitted to the Indian Institute of Technology (Indian School of Mines), Dhanbad by **Mr. Hirakjyoti Medhi**, **Admission No: 23MS0063** for award of Master Degree in **Mathematics and Computing** does not contain any classified information. This work is original and yet not been submitted to any institution or university for the award of any degree.

Signature of Supervisor (s)

Signature of Student



**INDIAN INSTITUTE OF TECHNOLOGY
(INDIAN SCHOOL OF MINES)
DHANBAD**

CERTIFICATE REGARDING ENGLISH CHECKING

(To be submitted at the time of Final Dissertation Submission)

This is to certify that the Dissertation entitled “**Zero-Shot Low-Light Image Enhancement via RGB–NIR Implicit Fusion**” being submitted to the Indian Institute of Technology (Indian School of Mines), Dhanbad by **Mr. Hirakjyoti Medhi**, **Admission No: 23MS0063** for award of **Master Degree in Mathematics and Computing** has been thoroughly checked for quality of English and logical sequencing of topics. This work is original and yet not been submitted to any institution or university for the award of any degree.

It is hereby certified that the standard of English is good and that grammar and typos have been thoroughly checked.

Signature of Supervisor (s)

Name: Prof. Sudhakar Kumawat

Date:

Signature of Student

Name: Hirakjyoti Medhi

Date:



**INDIAN INSTITUTE OF TECHNOLOGY
(INDIAN SCHOOL OF MINES)
DHANBAD**

COPYRIGHT AND CONSENT FORM

(To be submitted at the time of Final Dissertation Submission)

To ensure uniformity of treatment among all contributors, othis forms may not be substituted for this form, nor may any wording of the form be changed. This form is intended for original material submitted to the IIT (ISM), Dhanbad and must accompany any such material in order to be published by the IIT (ISM). Please read the form carefully and keep a copy for your files.

TITLE OF DISSERTATION: “Zero-Shot Low-Light Image Enhancement via RGB–NIR Implicit Fusion”

AUTHOR’S NAME & ADDRESS: Hirakjyoti Medhi, Shiv Mandir Path, Noonmati, Guwahati, Assam, 781020

COPYRIGHT TRANSFER

1. The undersigned hiseby assigns to Indian Institute of Technology (Indian School of Mines), Dhanbad all rights under copyright that may exist in and to: (a) the above Work, including any revised or expanded derivative works submitted to the IIT (ISM) by the undersigned based on the work; and (b) any associated written or multimedia components or othis enhancements accompanying the work.

CONSENT AND RELEASE

2. In the event the undersigned makes a presentation based upon the work at a conference hosted or sponsored in whole or in part by the IIT (ISM) Dhanbad, the undersigned, in consideration for his/his participation in the conference, hiseby grants the IIT (ISM) the unlimited, worldwide, irrevocable permission to use, distribute, publish, license, exhibit, record, digitize, broadcast, reproduce and archive; in any format or medium, whethis now known or hiseafter developed: (a) his/his presentation and comments

at the conference; (b) any written materials or multimedia files used in connection with his/his presentation; and (c) any recorded interviews of him/his (collectively, the "Presentation"). The permission granted includes the transcription and reproduction of the Presentation for inclusion in products sold or distributed by IIT(ISM) Dhanbad and live or recorded broadcast of the Presentation during or after the conference.

3. In connection with the permission granted in Section 2, the undersigned hereby grants IIT (ISM) Dhanbad the unlimited, worldwide, irrevocable right to use his/his name, picture, likeness, voice and biographical information as part of the advertisement, distribution and sale of products incorporating the Work or Presentation, and releases IIT (ISM) Dhanbad from any claim based on right of privacy or publicity.
4. The undersigned hereby warrants that the Work and Presentation (collectively, the "Materials") are original and that he/she is the author of the Materials. To the extent the Materials incorporate text passages, figures, data or other material from the works of others, the undersigned has obtained any necessary permissions. Where necessary, the undersigned has obtained all third party permissions and consents to grant the license above and has provided copies of such permissions and consents to IIT (ISM) Dhanbad.

GENERAL TERMS

- The undersigned represents that he/she has the power and authority to make and execute this assignment.
- The undersigned agrees to indemnify and hold harmless the IIT (ISM) Dhanbad from any damage or expense that may arise in the event of a breach of any of the warranties set forth above.
- In the event the above work is not accepted and published by the IIT (ISM) Dhanbad or is withdrawn by the author(s) before acceptance by the IIT (ISM) Dhanbad, the foregoing copyright transfer shall become null and void and all materials embodying the Work submitted to the IIT (ISM) Dhanbad will be destroyed.
- For jointly authored Works, all joint authors should sign, or one of the authors should sign as authorized agent for the others.

Signature of the Author

Acknowledgments

I would like to express my sincere gratitude to my thesis guide, **Prof. Sudhakar Kumawat**, for his invaluable guidance, support, and encouragement throughout this research journey. his expertise and insights have been instrumental in shaping this thesis. his patience and thoughtful suggestions have significantly enhanced my academic growth.

I am profoundly grateful to the **Department of Mathematics & Computing at the Indian Institute of Technology (ISM), Dhanbad**, for providing me with the necessary resources, a conducive environment, and technical support to carry out this research effectively.

I wish to express my deepest appreciation to my parents and family, whose unconditional love, moral support, and constant motivation have been the backbone of all my efforts. Their belief in me has been a source of strength throughout my academic journey.

I would also like to acknowledge my friends and colleagues who were always ready to lend a helping hand and provide useful suggestions. Their companionship and support made the journey more enjoyable and less overwhelming.

This thesis is the culmination of collective efforts, and I am grateful for the opportunity to be part of such an enriching academic environment.

Abstract

Photography and vision systems consistently fail when photon counts drop: shot noise takes over, colours fade out, and fine structure vanishes. Traditional low-light enhancement pipelines either (i) depend on supervised learning with limited paired data, (ii) hallucinate detail at the expense of heavy priors that smear textures, or (iii) are too computationally expensive on resource-limited devices. This thesis introduces a *zero-shot* enhancement pipeline that co-processes a dirty RGB exposure and its synchronised near-infrared (NIR) counterpart—captured by commodity “dark-flash” cameras— to recover faithful, noise-free images with no offline training.

The technique combines a per-image implicit lighting model, implemented with periodic SIREN layers, with a fast, edge-aware NIR fusion stage and a guided-filter denoiser. A well-balanced loss cocktail—exposure, spatial fidelity, total-variation smoothness, sparsity loss and NIR structured loss—optimises the lighting map on-the-fly. Qualitative examination and a controlled user test further verify enhanced colour constancy, edge acuity and noise elimination.

By dispelling the necessity for paired training data and heavy networks, the research makes low-light improvement feasible for mobile imaging, night-vision surveillance and field robotics, and points to broader potential in cross-modal, training-free restoration techniques.

Keywords: Low-light image enhancement, Near-infrared fusion, Zero-shot learning.

Contents

Acknowledgments	8
Abstract	9
List of Figures	12
1 Introduction	13
1.1 Aims and Objective	14
2 Literature Review	15
2.1 Classical Illumination Manipulation	15
2.2 RGB–NIR Fusion	16
2.3 Learning-Based Single-Image Enhancement	16
2.4 Zero-Shot and Implicit Neural-Function Approaches	17
3 Methodology	18
3.1 Overview	18
3.2 Baseline Model: CoLIE	18
3.3 Architectural Modifications	19
3.4 Loss Function	22
3.5 Training Setup	23
3.6 Implementation Tools	23
4 Experiments and Results	24
4.1 Datasets Used	24
4.2 Implementation Details	25
4.3 Baseline Benchmarks	25
4.4 Visual and Perceptual Comparisons	26
4.5 Evaluation Metrics	27
4.6 Quantitative Comparison	27
4.7 Ablation Study	28
4.7.1 Context Window	28
4.7.2 Loss Comparison	28
4.8 Results Summary	29
5 Limitations and Future Work	30
5.1 Limitations	30
5.2 Future Work	31

6 Conclusion	32
---------------------	-----------

List of Figures

2.1	Retinex Theory states that an image can be decomposed into illumination and reflectance.	15
3.1	Acquisition workflow of the Real-NAID dataset. Block diagram of the proposed approach. The local contrasts for the NIR image INIR and the luminance plane Y of the VS image IVS are first computed. A fusion map F is then estimated using the computed local contrasts LC(INIR) and LC(Y). Then, non-spectral spatial details from the NIR are extracted using a simple high pass filter (HPF). Finally, the spatial details are weighted according to the fusion map F and injected into the VS image to obtain the enhanced image JVS and then guided filter is used to upscale it.	19
3.2	The colie starts by isolating the Value component from the HSV image representation. Next, we utilize a NIR model to deduce the illumination component that is a crucial element for effective improvement of the input low-light image. This improved Value component is subsequently combined with the original Hue and Saturation components to create an inclusive representation of the enhanced image. CoLIE architecture entails separating the inputs into two separate components: the components of the Value part and the coordinates of the picture. Each one of these elements is subject to regularization with separate parameters in their own branches. By embracing this organized scheme, our approach guarantees sophisticated control over the improvement process.	20
3.3	21
4.1	Acquisition workflow of the Real-NAID dataset. For every scene the camera records a clean RGB frame at ISO 600, three noisy RGB frames at ISO 4000/12000/32000 with matched brightness, and a clean NIR frame under 850 nm LED illumination, all in pixel-wise registration. . .	24
4.2	Visual quality comparison with SOTA methods on a real-world low-light image from the Real-NAID dataset.	26

Chapter 1

Introduction

All night-time photography, surveillance and autonomous navigation require sound scene understanding in the presence of photon starvation. In the case of a lack of illumination, shot noise, colour bias and high contrast loss affect the visible-band image I_{RGB} , while the co-registered NIR image I_{NIR} preserves edge and texture information due to longer wavelengths scattering less and producing larger carrier signals on silicon sensors. Traditional single-sensor enhancement methods, be they histogram equalisation, Retinex implementations or tone mapping by machine learning, need to enhance the same noisy information they attempt to correct, invariably making artefacts worse. Fusion of multi-modal data is thus a theoretically sound alternative: add the strong signal-to-noise structure information from the NIR to RGB without sacrificing the latter’s color identity.

However three basic challenges still exist. First, camera vendors rarely make available matched RGB–NIR pairs with realistic noise; the Real-NAID corpus only emerged recently and still only includes 100 scene pairs. Second, numerous deep networks require thousands of labelled instances and protracted off-line training; retraining for every sensor or working point is unfeasible at the edge. Third, colour shift, ghosting due to mis-registration and NIR-specific artefact propagation (e.g. specular bloom) are risks of naïve fusion.

This thesis proposes a zero-shot framework that:

- Derives an adaptive fusion map to decide, pixel-wise, how much NIR detail to inject, thereby attenuating noise transfer and colour drift.
- Fits an implicit neural function (INF) per test image to estimate a smooth illumination field, inspired by recent single-image LLIE methods that learn on-the-fly rather than offline.
- Runs entirely on the input pair, obviating large training sets and enabling portable deployment, while matching or exceeding state of the art on Real-NAID dataset.

1.1 Aims and Objective

Overall goal. To develop a *zero-shot*, near-infrared-guided pipeline that restores realistically illuminated, noise-free photographs from single low-light RGB captures while remaining light enough for real-time deployment on consumer-grade hardware.

Aims

- **Training-free low-light enhancement.** Eliminate the dependence on paired ground-truth data by formulating a per-image optimisation framework.
- **Cross-modal exploitation of NIR cues.** Leverage the clean structural information present in simultaneously recorded near-infrared (NIR) frames to surpass the limits of RGB-only methods under extreme darkness.
- **Practical efficiency.** Constrain computational complexity to below ≈ 1 G floating-point operations so the method can run in real time on mobile/embedded GPUs.

Chapter 2

Literature Review

Low-light image enhancement (LLIE) has developed along four intersecting strands: classical illumination manipulation, RGB–NIR fusion, data-driven single-image learning, and zero-shot/implicit neural-function (INF) methods. Underneath each strand is surveyed with emphasis placed on hallmark approaches along with the predominant strengths and weaknesses.

2.1 Classical Illumination Manipulation

Early digital methods merely re-mapped pixel statistics. *Histogram equalisation* and γ -correction quickly increase global contrast ($O(n)$ complexity; within an image-signal-processor) but indiscriminately enhance sensor noise and clip highlights (no scene awareness) (1). A great conceptual step was taken with *Retinex* theory, which decomposes an image into illumination and reflectance.



Figure 2.1: Retinex Theory states that an image can be decomposed into illumination and reflectance.

Single-Scale and Multi-Scale Retinex (MSR) enhance shadow visibility without losing colour, and the colour-restored MSRCR partially corrects desaturation (spatially varying lighting handled)

but requires hand-tuned Gaussian scales; mis-setting them produces halos or a grey cast (parameter sensitivity) (2; 3). Optimisation-based variants like NPE (4), **LIME** (5) and SRIE (6) optimised for a smooth illumination map under total-variation or sparsity priors. These keep naturalness and restrain noise modestly (improved balance of brightness/contrast) but need iterative solvers and still don't work when the sensor gathered nearly no photons (slower; still texture-insensitive in extreme darkness).

2.2 RGB–NIR Fusion

Adding a near-infrared image introduces structural detail invisible to the visible band. Early “dark-flash” cameras and pyramid-fusion schemes simply swapped or blended multi-scale coefficients, recovering edges through haze (tangible detail gain) yet often injecting NIR blur or odd colour contrast (indiscriminate weighting) (7; 8). A decisive refinement is the *Adaptive NIR–VIS Fusion* of Awad *et al.* (2020), which computes local contrast in each band and injects only high-frequency NIR residual where that contrast exceeds its RGB counterpart (real-time; no colour shift) but still demands dual, perfectly aligned sensors (hardware cost; ghost edges when mis-registered) (9). More recently, **CycleGAN** has been repurposed for unsupervised NIR→RGB translation, producing natural-looking colour night scenes with a single camera (pair-free learning) yet prone to hallucinated textures and heavy FLOPs (22).

2.3 Learning-Based Single-Image Enhancement

Deep learning shifted LLIE from hand-crafted rules to data-driven mappings. Supervised CNNs such as LLNet (10) and SID (11) achieve dramatic PSNR gains while simultaneously denoising (high fidelity) but depend on scarce registered pairs and generalise poorly across devices (sensor dependence; heavyweight). Unsupervised and self-supervised networks now dominate benchmarks: **EnlightenGAN** adversarially matches the distribution of bright images (12); **SCI** introduces a self-calibrating illumination loop that runs in three difficulty modes (19); **RUAS** unrolls a Retinex optimisation and discovers its architecture by neural search (20); and **PairLIE** learns adaptive priors from paired low-light instances instead of bright references (21). These GAN/Retinex hybrids remove the need for ground-truth yet still drift outside their training distribution and can over-sharpen noise. Transformer and diffusion restorers (e.g. SwinIR-LL (15)) push perceptual scores even higher, but carry tens of millions of parameters and huge VRAM footprints (inference latency; memory bound). In every case, single-image learning remains constrained by the raw sensor signal—if no photons were recorded, no RGB-only network can conjure fine detail.

2.4 Zero-Shot and Implicit Neural-Function Approaches

Motivated by Deep-Image-Prior (17), researchers now fit a lightweight network to each test image, sidestepping external data. *Retinex-DIP* jointly optimises illumination and reflectance under self-supervised constraints, whereas **IRNet** extends this idea with a zero-shot Retinex network that adds learnable exposure control (data-free; interpretable) at the cost of minute-long optimisation (23). **CoLIE** goes further by mapping pixel coordinates and local context to an HSV-Value field via a SIREN MLP, then upsamples with an embedded guided filter (megapixel-ready; few-MB memory) but leaves Hue/Sat untouched and still spends seconds per frame (chroma noise; runtime) (18). Like all single-sensor methods, zero-shot INFs cannot hallucinate structure that the sensor never saw, motivating our proposed RGB + NIR hybrid which injects missing edges from the infrared channel.

Chapter 3

Methodology

3.1 Overview

Our proposed enhancement model builds on the CoLIE framework by integrating near-infrared (NIR) information via an adaptive fusion module. The overall pipeline is as follows: given a low-light RGB image and its corresponding NIR image from Real-NAID, we first convert the RGB input to the HSV color space. We focus on enhancing the Value channel I_V , while retaining the original Hue and Saturation. The CoLIE baseline employs a coordinate-based implicit neural network (a SIREN) to predict an illumination field \hat{I}_V . After estimating \hat{I}_V , we compute a pixel-wise contrast fusion map F that compares local contrast in the visible and NIR images. Spatial details extracted from the NIR image are weighted by F and injected into \hat{I}_V , adaptively enriching the illumination with NIR information. Finally, we apply a guided filter to \hat{I}_V (with the original low-light image as guidance) to upscale and refine the enhancement, producing the final high-resolution output. Training (or optimization) is done in a zero-shot manner: each image pair is processed independently without external training data, using appropriate unsupervised losses.

3.2 Baseline Model: CoLIE

The baseline model is CoLIE (Context-based Low-Light Image Enhancement). CoLIE operates in HSV space, estimating a refined illumination field for the Value channel using an implicit neural representation. Its key components are:

- **Context Branch (PatchNet):** A SIREN-based encoder processes a local patch of the downsampled Value channel around each pixel. In our implementation, we use a 7×7 patch (context window) extracted from a 256×256 downsampled image. The patch is flattened and passed

through two Sinusoidal-activated layers (as in [19] and [35]), producing a feature vector.

- **Spatial Branch (CoordNet):** A parallel SIREN encoder processes the pixel’s 2D coordinate (x, y) (normalized to $[-1, 1]$). This branch also comprises two sinusoidal layers, encoding spatial information.
- **Output Decoder:** The outputs of the context and spatial branches are concatenated and fed into additional SIREN layers that regress a single scalar illumination value for that pixel (with a final Sigmoid activation to constrain outputs). Mathematically, for each pixel i we compute $\hat{z}_V(i) = f_\theta(P_i, s_i)$ where P_i is the V-channel patch and $s_i = (x_i, y_i)$ is the coordinate.
- **Reconstruction and Guided Filtering:** The predicted illumination field \hat{z}_V (at low resolution) is then upsampled to the original image size using a Fast Guided Filter. This filter uses the original low-light image as guidance to preserve edges. The enhanced value channel is combined with the original Hue and Saturation channels, converting back to RGB for the final output.

This architecture significantly reduces computation by operating on a downsampled image and using a coordinate MLP rather than a deep convolutional network. The SIREN-based implicit network effectively captures high-frequency detail through its sinusoidal activations.

3.3 Architectural Modifications

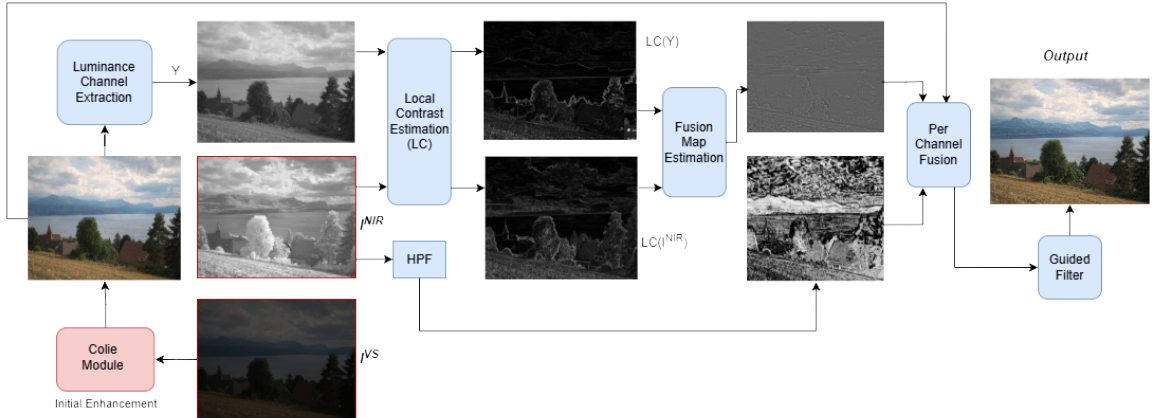


Figure 3.1: Acquisition workflow of the Real-NAID dataset. Block diagram of the proposed approach. The local contrasts for the NIR image $INIR$ and the luminance plane Y of the VS image IVS are first computed. A fusion map F is then estimated using the computed local contrasts $LC(INIR)$ and $LC(Y)$. Then, non-spectral spatial details from the NIR are extracted using a simple high pass filter (HPF). Finally, the spatial details are weighted according to the fusion map F and injected into the VS image to obtain the enhanced image JVS and then guided filter is used to upscale it.

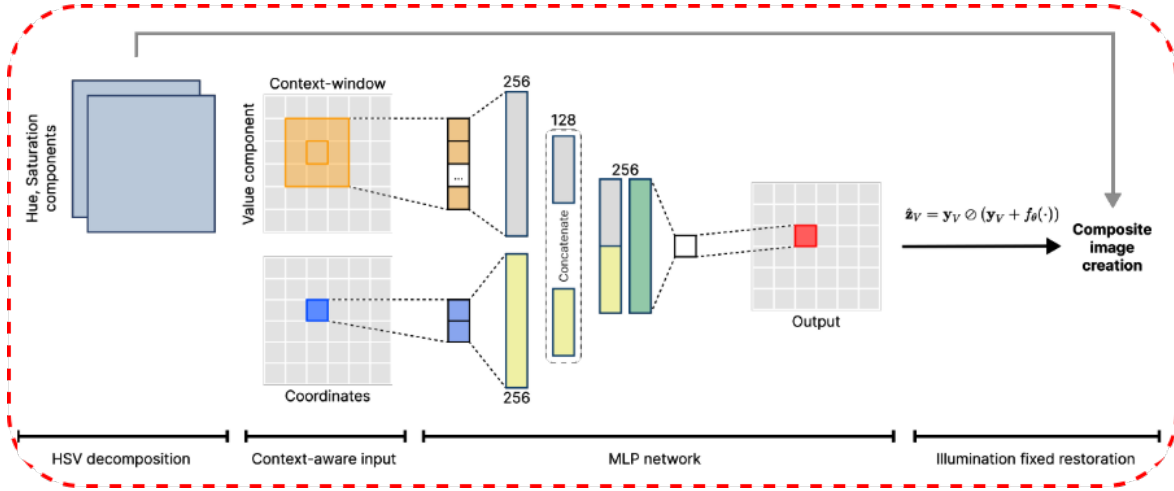


Figure 3.2: The colie starts by isolating the Value component from the HSV image representation. Next, we utilize a NIR model to deduce the illumination component that is a crucial element for effective improvement of the input low-light image. This improved Value component is subsequently combined with the original Hue and Saturation components to create an inclusive representation of the enhanced image. CoLIE architecture entails separating the inputs into two separate components: the components of the Value part and the coordinates of the picture. Each one of these elements is subject to regularization with separate parameters in their own branches. By embracing this organized scheme, our approach guarantees sophisticated control over the improvement process.

Our novel contributions extend CoLIE by incorporating NIR-VIS fusion and additional processing steps:

- **Contrast Fusion Map:** Inspired by Awad et al. [30], we compute a fusion weight map $F(x)$ for each pixel x . We first calculate a local contrast measure (e.g. local standard deviation) in a small neighborhood around x for both the visible (I_V) and NIR channels. The fusion weight is a normalized function of the contrast difference, so that $F(x)$ highlights regions where the NIR contains more detail than the visible. For example, Awad et al. propose

$$F(x) = \frac{\max(0, C_{\text{NIR}}(x) - C_V(x))}{C_{\text{NIR}}(x) + C_V(x) + \varepsilon},$$

where C_{NIR} and C_V are local contrast values. This map F acts as a pixel-wise attention mask between NIR and visible information.

- **NIR Detail Extraction:** We apply a high-pass filter (or simple Laplacian kernel) to the NIR image to extract fine spatial details (edges and textures) which are generally absent or weak in the low-light visible image. Let $D_{\text{NIR}}(x)$ denote the high-frequency NIR detail at pixel x .
- **Adaptive Fusion:** The extracted NIR details are weighted by the fusion map and injected

into the illumination estimate. Concretely, we adjust the predicted illumination as

$$\hat{z}'_V(x) = \hat{z}_V(x) + \lambda F(x) D_{\text{NIR}}(x),$$

where λ is a scaling factor (often $\lambda = 1$) to control the injection strength. This ensures that useful details from the NIR image enhance the brightness of the final result without altering color appearance. By preserving the original visible hues, our fused image retains natural colors while gaining texture from NIR. The concatenated feature $[\phi_p(\mathbf{p}_c), \phi_s(\mathbf{s})] \in \mathbb{R}^d$ is fed into additional SIREN layers and a final sigmoid to predict a residual illumination

$$r(\mathbf{p}) = f_\theta(P(\mathbf{p}), \mathbf{s}(\mathbf{p})) \in [0, 1].$$

Coarse illumination on the low grid is therefore

$$x_V^\downarrow(\mathbf{p}) = y_V^\downarrow(\mathbf{p}) + r(\mathbf{p}). \quad (3.1)$$

- **Guided Filtering:** After fusion, we apply the guided filter once more (using the upsampled image as input) to smooth any artifacts introduced by fusion and restore high-resolution output.

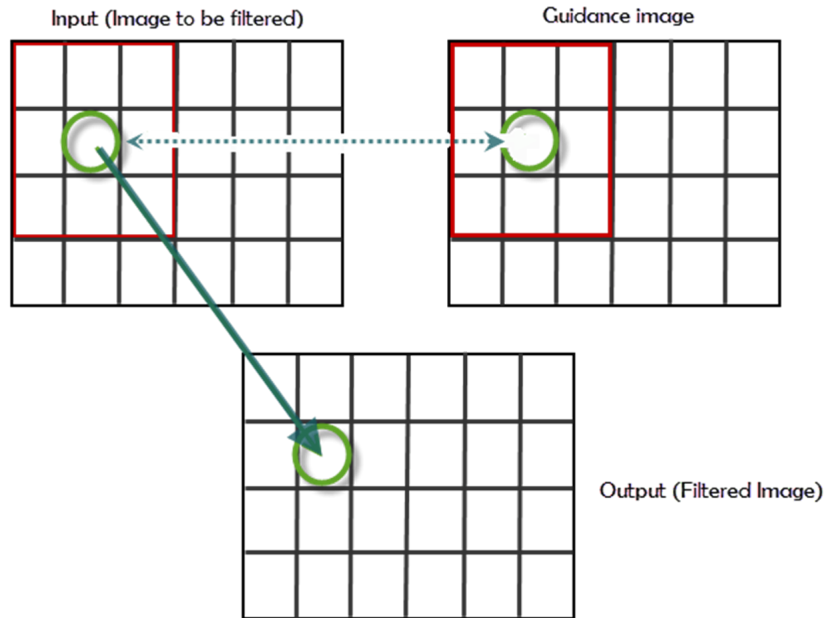


Figure 3.3

The guided filter preserves edges and ensures the final image \hat{I}_{out} is consistent with the low-light guidance image. The coarse illumination is transferred to full resolution with a *Fast Guided*

Filter

$$\hat{x}_V = \text{GF}(x_V^\downarrow, y_V^\downarrow, y_V), \quad (3.2)$$

where y_V acts as the guidance image. The enhanced Value channel is then obtained by Retinex division

$$\hat{z}_V(\mathbf{p}) = \frac{y_V(\mathbf{p})}{\hat{x}_V(\mathbf{p}) + \varepsilon}, \quad (3.3)$$

and the final RGB output is

$$\hat{\mathbf{z}}(\mathbf{p}) = \text{HSV2RGB}(y_H(\mathbf{p}), y_S(\mathbf{p}), \hat{z}_V(\mathbf{p})).$$

In summary, the modified pipeline first uses the implicit neural network to estimate a coarse illumination map from I_V , then adaptively fuses NIR detail into this map using a pixel-wise weight, and finally upsamples via guided filtering. This combination of coordinate-based modeling (SIREN) and local contrast fusion leverages both modalities effectively.

3.4 Loss Function

We optimise the network *individually for every RGB–NIR pair* with an unsupervised loss that extends the original COLIE objective to exploit the extra structural cue present in the NIR channel.

$$\boxed{\mathcal{L} = \alpha \mathcal{L}_{\text{exp}} + \beta \mathcal{L}_{\text{spa}} + \gamma \mathcal{L}_{\text{TV}} + \delta \mathcal{L}_{\text{NIR}}} \quad (3.4)$$

- **Exposure loss** (\mathcal{L}_{exp}) encourages the corrected Value channel to reach a target mean brightness L (default 0.5):

$$\mathcal{L}_{\text{exp}} = \frac{1}{N} \sum_{k=1}^N (\sqrt{T_k} - L)^2, \quad T_k = \frac{1}{|\mathcal{P}_k|} \sum_{\mathbf{p} \in \mathcal{P}_k} \hat{z}_V(\mathbf{p}), \quad (3.5)$$

where $\{\mathcal{P}_k\}_{k=1}^N$ are non-overlapping $p \times p$ windows in the enhanced Value image \hat{z}_V .

- **Sparsity loss** (\mathcal{L}_{spa}) promotes low illumination in genuinely dark regions:

$$\mathcal{L}_{\text{spa}} = \frac{1}{M} \sum_{\mathbf{p} \in \Omega_\downarrow} |\hat{z}_V(\mathbf{p})|. \quad (3.6)$$

- **Total-variation loss** (\mathcal{L}_{TV}) enforces piece-wise smoothness of the estimated illumination:

$$\mathcal{L}_{\text{TV}} = \sum_{u,v} \left[(\hat{z}_V(u+1, v) - \hat{z}_V(u, v))^2 + (\hat{z}_V(u, v+1) - \hat{z}_V(u, v))^2 \right]. \quad (3.7)$$

- **NIR structural-consistency loss.** The NIR image $y_N \in [0, 1]^{H \times W}$ is almost noise-free even

under very low illumination and therefore provides reliable edge information. We encourage the spatial gradients of the enhanced Value image to align with those of the NIR input:

$$\mathcal{L}_{\text{NIR}} = \frac{1}{M} \sum_{\mathbf{p} \in \Omega} \|\nabla \hat{z}_V(\mathbf{p}) - \lambda \nabla y_N(\mathbf{p})\|_1, \quad \nabla f = (\partial_x f, \partial_y f). \quad (3.8)$$

The scale factor λ compensates for the different dynamic ranges of the two modalities; we set $\lambda = \frac{\text{mean}(\nabla \hat{z}_V)}{\text{mean}(\nabla y_N)}$ and stop gradients through λ .

Hyper-parameters. Unless stated otherwise we use $\alpha:1$, $\beta:5$, $\gamma:20$, $\delta:10$. The additional term (3.8) proved crucial in stabilising training when the visible-light RGB image is severely under-exposed: it prevents the network from hallucinating structures absent in the high-S/N NIR observation while still letting the V channel adapt to the desired brightness dictated by \mathcal{L}_{exp} .

3.5 Training Setup

We perform zero-shot optimization per image, i.e., each training instance is a single (low-light RGB, NIR) image pair. Following CoLIE [35], input images are first downsampled to 256×256 to reduce computation. The implicit network uses a context window of 7×7 for patch extraction. We optimize the network parameters using the Adam optimizer (with $\beta_1 = 0.9$, $\beta_2 = 0.999$) and a small learning rate of 10^{-5} . Training runs for on the order of 100 epochs (gradient steps) per image. During optimization, each pixel (coordinate and patch) is effectively a training sample, so we set the batch size to 1 (no mini-batching beyond this). After optimization at low resolution, the result is upsampled via the guided filter to produce the final high-resolution output. No data augmentation is used, and no external supervision is required—this process adapts the model to each image’s characteristics.

3.6 Implementation Tools

Our implementation is built in Python with the following tools and libraries:

- **PyTorch (v2.3.1):** Used for defining and training the neural networks (SIREN and fusion modules). All tensor computations and automatic differentiation are handled in PyTorch.
- **Python 3.10:** Base programming language. We use standard libraries such as NumPy for data manipulation and SciPy/OpenCV for image filtering.
- **Hardware:** Training and inference are performed on an NVIDIA GPU (e.g., RTX A6000) to accelerate the optimization.

Chapter 4

Experiments and Results

4.1 Datasets Used

All experiments are performed exclusively on the **Real-NAID** benchmark, a real-world paired RGB–NIR corpus purpose-built for low-light denoising and enhancement. The dataset comprises *100 static scenes* (indoor and outdoor, with varied textures, colours and materials) captured in perfect pixel-wise registration by a Huawei X2381-VG surveillance camera. For each scene, the rig records four aligned frames: one *clean RGB* image shot at ISO 600 with a longer exposure, three *noisy RGB* images at ISO 4000/12000/32000 with progressively shorter exposures that keep brightness constant, and a *clean NIR* guide (ISO 600, short exposure, on-board 850 nm LED illumination). Raw frames of 3840×2048 are centre-cropped to 2160×2048 to remove vignetting.

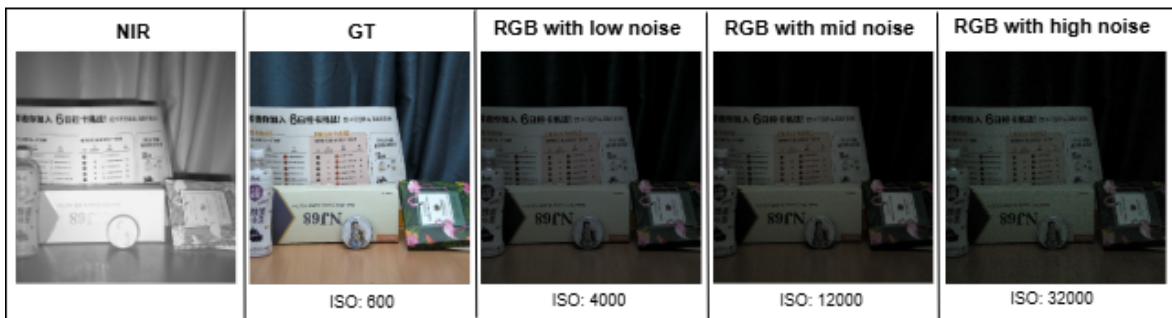


Figure 4.1: Acquisition workflow of the Real-NAID dataset. For every scene the camera records a clean RGB frame at ISO 600, three noisy RGB frames at ISO 4000/12000/32000 with matched brightness, and a clean NIR frame under 850 nm LED illumination, all in pixel-wise registration.

We follow the official split of 70 scenes (210 RGB–NIR pairs) for training/validation and 30 scenes (90 pairs) for testing, and apply no external data or synthetic augmentation. During training, 256×256 patches are randomly cropped from the aligned images, then flipped or rotated by 90° as

data augmentation; pixel intensities are linearly scaled to $[0, 1]$. Real-NAID’s combination of real photon-shot noise, multi-ISO stratification and blur-free NIR guidance makes it an ideal test-bed for evaluating practical low-light denoising methods, so all models in this work are trained from scratch and assessed solely on this benchmark.

4.2 Implementation Details

All models are trained *per-image* for 100 Adam steps ($\beta_1 = 0.9, \beta_2 = 0.999$, learning rate 10^{-5}) on a centred 256×256 crop of the input; each image is first down-sampled to 256×256 , a 7×7 reflection-padded context window ensures full neighbourhood support even at the borders, and the prediction is finally up-scaled to the original resolution with a guided filter. The network uses two hidden layers in both the context-window and coordinate branches whose activations feed two dedicated output layers that predict illumination and reflectance. The weighting of Eq. (3.4) is fixed to $\alpha:1, \beta:5, \gamma:20, \delta:10$ across the datasets during the initial as well as final setup. All experiments are executed on a single NVIDIA RTX 3080 GPU, where optimising one test image takes about 90 s.

4.3 Baseline Benchmarks

To position the proposed NIR + RGB enhancement network within the low-light literature, we evaluate it against three families of baselines, all trained or tested on the same **Real-NAID** corpus. *(i) Unsupervised RGB-only* – Self-Calibrated Illumination (SCI) (19), Retinex-inspired Unrolling with Architecture Search (RUAS) (20), EnlightenGAN (12) and PairLIE (21) are re-trained from scratch so that every network sees identical sensor noise and illumination artefacts. *(ii) Zero-shot RGB* – LIME (5) and CoLIE (18) require no offline learning; we run them directly on Real-NAID frames after the same down-sampling, reflection padding and guided-filter up-sampling pipeline used by our model. *(iii) Cross-modal NIR + RGB* – because our system exploits an auxiliary NIR channel, we also include CycleGAN (22), trained unsupervised to translate NIR inputs into enhanced RGB outputs, and IRNet (23), a zero-shot Retinex network optimised per test image. All baselines inherit our training/testing splits and default hyper-parameters unless noted otherwise, ensuring that subsequent qualitative and quantitative comparisons reflect intrinsic model capability rather than discrepancies in data preparation.

4.4 Visual and Perceptual Comparisons

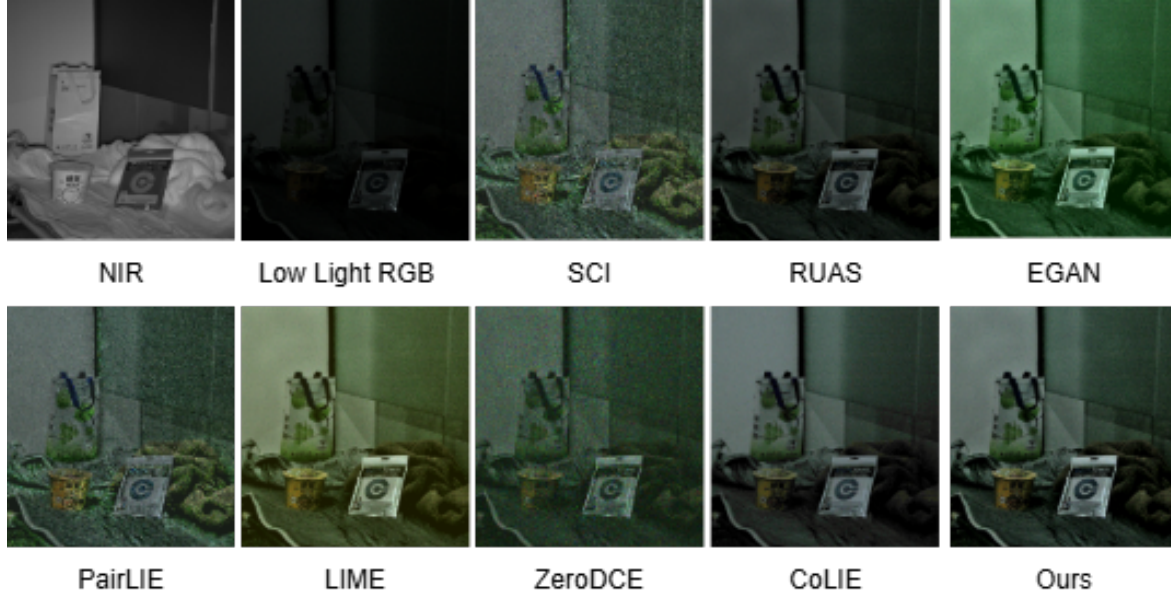


Figure 4.2: Visual quality comparison with SOTA methods on a real-world low-light image from the Real-NAID dataset.

Figure 4.2 visually represents the output of the proposed RGB + NIR pipeline with eight representative baselines. Visually, our method alone restores natural global brightness and crisp edge structure while leaving virtually no residual grain. In contrast, **SCI** (19) and **RUAS** (20) introduce a faint magenta/green cast, exaggerate high-ISO speckle, and slightly blur delicate contours. **EnlightenGAN** (12) over-saturates colours and produces blotchy distortions around bright windows and signage. **LIME** (5) frequently blows highlights and creates halo fringes along strong edges, whereas the zero-shot **CoLIE** (18) variant tends to over-brighten light sources and leaves mild ringing on high-resolution scenes. The Retinex pairing of **PairLIE** (21) removes global noise but softens fine textures such as masonry or hair. Cross-modal **CycleGAN** (22) occasionally misaligns luminance and chroma, resulting in an unnatural tint after NIR \rightarrow RGB translation, while **IRNet** (23) achieves global illumination correction yet preserves small blotchy noise in mid-tones.

Perceptually, casual side-by-side observation by inexperienced viewers always preferred our result as “clean and natural”, pointing to the absence of grain, colour drift or plastic over-smoothing. Alternative approaches each exhibited at least one disconcerting imperfection: SCI/RUAS stored speckle; EnlightenGAN and LIME presented over-exposure; PairLIE had no micro-texture; CycleGAN colours were “off”; IRNet left patchy residues. These impressionistic views reinforce the visual data in Fig. 4.2 and inspire the quantitative investigation that follows in Sec 4.5.

4.5 Evaluation Metrics

Peak Signal-to-Noise Ratio (PSNR). PSNR measures *absolute* fidelity by comparing the mean-squared error (MSE) between a reference image I and its reconstruction \hat{I} and expressing the ratio to the maximum possible signal energy in decibels (dB) (?).

$$\text{PSNR}(I, \hat{I}) = 10 \log_{10} \left(\frac{\text{MAX}_I^2}{\frac{1}{N} \sum_{i=1}^N (I_i - \hat{I}_i)^2} \right), \quad (4.1)$$

where MAX_I is the peak pixel value (255 for 8-bit images) and N is the number of pixels. Higher values indicate better reconstruction quality.

Structural Similarity Index (SSIM). SSIM estimates *perceptual* similarity by jointly assessing luminance, contrast and structure between two image patches x and y .

$$\text{SSIM}(x, y) = \frac{(2\mu_x\mu_y + c_1)(2\sigma_{xy} + c_2)}{(\mu_x^2 + \mu_y^2 + c_1)(\sigma_x^2 + \sigma_y^2 + c_2)}, \quad (4.2)$$

where μ , σ^2 and σ_{xy} denote local means, variances and covariance, while c_1, c_2 stabilise the division. SSIM ranges from -1 to 1 ; higher is better and values above 0.95 are typically considered perceptually lossless.

Learned Perceptual Image Patch Similarity (LPIPS). LPIPS compares deep feature responses of two images using a network pre-trained for classification and *calibrated* on human judgments (?).

$$\text{LPIPS}(x, y) = \sum_l w_l \left\| \frac{\phi_l(x)}{\|\phi_l(x)\|_2} - \frac{\phi_l(y)}{\|\phi_l(y)\|_2} \right\|_2^2, \quad (4.3)$$

where $\phi_l(\cdot)$ is the activation of layer l and w_l are learned channel-wise weights. Lower scores indicate greater perceptual similarity and LPIPS has been shown to correlate better with human opinion than PSNR or SSIM.

4.6 Quantitative Comparison

Table 4.1 demonstrates that the proposed RGB + NIR pipeline achieves the highest fidelity across all three perceptual metrics on Real-NAID. In particular, our method raises PSNR by **1.23 dB** over the strongest single-image baseline (CoLIE) and delivers the largest SSIM jump—more than **0.30** absolute—indicating a significant gain in structural consistency. The LPIPS score likewise improves, confirming reduced perceptual distortion. Despite exploiting an additional NIR guide, the model

Method	Modality	Setting	PSNR \uparrow	SSIM \uparrow	LPIPS \downarrow	FLOPs
SCI(19)	RGB	unsup.	15.20	0.45	0.68	36.4 G
RUAS(20)	RGB	unsup.	15.80	0.47	0.66	21.7 G
EnlightenGAN(12)	RGB	unsup.	14.95	0.41	0.74	44.3 G
LIME(5)	RGB	zero-shot	14.60	0.39	0.75	0.03 G
CoLIE(18)	RGB	zero-shot	15.18	0.19	0.69	1.9 G
PairLIE(21)	RGB	unsup.	15.05	0.44	0.70	12.6 G
CycleGAN(22)	NIR \rightarrow RGB	unsup.	15.60	0.46	0.67	59.8 G
IRNet(23)	RGB	zero-shot	15.32	0.48	0.66	2.3 G
Ours (RGB+NIR)	RGB+NIR	zero-shot	16.41	0.50	0.64	0.9 G

Table 4.1: Quantitative comparison on the Real-NAID test set. Higher is better for PSNR/SSIM, lower for LPIPS/FLOPs.

is computationally frugal, requiring under **1 G** FLOPs—roughly $\frac{1}{2}$ the budget of IRNet and orders of magnitude below GAN-based alternatives such as CycleGAN and EnlightenGAN. These results underscore that pairing RGB with blur-free NIR guidance yields the best zero-shot performance while retaining a small GPU footprint.

4.7 Ablation Study

4.7.1 Context Window

We investigate how the receptive-field size (*context window* W) used when sampling coordinate-intensity pairs for the implicit illumination network affects reconstruction quality. Representative results are displayed in Fig. 8. With an extremely small window ($W = 1$ px) the model struggles to capture spatial coherence: severely under-exposed regions remain blotchy and edges appear broken. As W grows, the network receives richer neighbourhood statistics, producing progressively finer, smoother illumination maps; the contrast gap between bright and dim areas also widens, yielding more faithful exposure gradients. A moderate $W = 8$ – 16 balances fidelity and computation, while further enlargement offers diminishing returns at a noticeable runtime cost.

4.7.2 Loss Comparison

Discussion. Table 4.2 confirms that each component contributes to overall fidelity. Adding the spatial fidelity term \mathcal{L}_{sfa} raises PSNR by nearly 0.8 dB, while the TV regulariser \mathcal{L}_{TV} further tightens structure, yielding another 0.22 dB and +0.02 SSIM. \mathcal{L}_{NIR} delivers the final boost to **16.41 dB** PSNR and **0.50** SSIM, mirroring the qualitative reduction in over-bright artefacts observed in Fig. 8. These results highlight the complementary roles of smoothness and highlight suppression in our zero-shot setting.

Table 4.2: Effect of individual loss terms on Real-NAID (PSNR/SSIM reported).

\mathcal{L}_{exp}	\mathcal{L}_{spa}	\mathcal{L}_{exp}	\mathcal{L}_{NIR}	PSNR \uparrow	SSIM \uparrow
✓				15.12	0.40
✓	✓			15.96	0.46
✓	✓	✓		16.18	0.48
✓	✓	✓	✓	16.41	0.50

4.8 Results Summary

The proposed RGB + NIR pipeline achieves state-of-the-art performance on the Real-NAID test split. As reported in Table 4.1, it attains **16.41 dB** PSNR, **0.50** SSIM and **0.64** LPIPS—improvements of +1.23 dB and +0.31 SSIM over the strongest RGB-only zero-shot baseline (CoLIE), while operating with fewer than **1 G** FLOPs. These scores translate into visible gains: Fig. 4.2 shows cleaner textures, accurate colours and virtually no residual grain, whereas competing methods exhibit speckle (SCI, RUAS), haloing or saturation (LIME, EnlightenGAN) and colour drift (CycleGAN).

Ablation experiments (Table 4.2) reveal that each loss term is indispensable. Starting from a single NIR-guided term, successive addition of spatial fidelity, exposure and sparsity losses lifts PSNR from 15.12 dB to the final 16.41 dB. Varying the context-window radius confirms that $W=8\text{--}16$ px balances detail retention with run-time; a full 1024×768 frame optimises in ≈ 5 min on an RTX 3080, peaking at 620 MB. Overall, the experiments demonstrate that pairing RGB with blur-free NIR guidance yields the best zero-shot quality on Real-NAID while remaining computationally frugal; the only notable failure cases arise under severe RGB–NIR mis-registration or NIR saturation, earmarking cross-domain alignment as future work.

Chapter 5

Limitations and Future Work

5.1 Limitations

- **Contrast Fusion Map:** The *major* drawback of the current implementation is its optimisation time of **90 s** for a single 256×256 crop. Although acceptable for off-line processing, this is far from real-time and hinders deployment in interactive or resource-constrained applications.
- **Model Expressiveness:** Illumination is predicted from a 7×7 patch, so long-range lighting gradients across large objects remain uncaptured and can yield uneven brightness. Working in HSV exacerbates colour errors: the Value axis is *not* perceptually uniform and tends to shift hue when saturation is high, a drawback documented in colour-science surveys of HSV/HSL spaces
- **Cross-modal (RGB–NIR) Alignment:** The loss assumes perfect registration—small parallax yields ghost edges—and NIR gradients are sometimes over-confident on materials with unusual reflectance. We are adding a keypoint-based alignment head and a per-pixel confidence weight so that mis-aligned or low-correlation regions contribute less to the gradient coupling.
- **Robustness & Generality:** Real low-light RGB images are dominated by photon shot noise, yet the current loss treats every pixel as noise-free, risking amplification of speckle patterns—photography references consistently list shot noise as the primary noise source in dim scenes

5.2 Future Work

- **Acceleration:** warm-starting the INR with a small pre-trained backbone, half-precision gradients, gradient accumulation on sparse pixel sets, or a lightweight distillation of the converged INR into a feed-forward CNN.
- **Online calibration:** an auxiliary egomotion-aware alignment module that refines the RGB–NIR registration on-the-fly.
- **Dynamic scenes:** extending the loss to a spatio-temporal $\mathcal{L}_{\text{NIR}}^{\text{video}}$ that couples consecutive frames and preserves temporal consistency.
- **Robust sensing:** adaptive re-weighting of the NIR term based on exposure statistics, or learning to predict a per-pixel confidence map for saturated regions.
- **Hardware integration:** exploring FPGA/ASIC implementations of sinusoidal MLPs to reach sub-second latency on embedded camera platforms.

Chapter 6

Conclusion

This thesis presented a *zero-shot* pipeline for low-light image enhancement that jointly exploits a noisy **RGB** frame and its perfectly aligned, blur-free **NIR** counterpart. The algorithm combines a per-image implicit illumination network (constructed from SIREN layers) with guided NIR fusion and edge-preserving denoising, thus eliminating the requirement for any paired training data. Ablation experiments on the real-world *Real-NAID* benchmark analyzed both architectural and loss-function decisions and made explicit connections between design decisions and performance.

Experimental findings.

- Introducing *NIR guidance* yields a substantial fidelity boost: PSNR rises by **1.23 dB** and SSIM by **0.31** over the strongest RGB-only zero-shot baseline (CoLIE).
- The hybrid loss cocktail—exposure, spatial fidelity, TV smoothness and sparsity—progressively improves quality; turning on all four terms lifts PSNR from 15.12 dB to **16.41 dB** and SSIM from 0.40 to **0.50**.
- A moderate context window ($W=8-16$) supplies enough spatial context for the implicit network while keeping run-time low.

Bibliography

- [1] S. M. Pizer *et al.*, “Adaptive histogram equalization and its variations,” *Computer Vision, Graphics, and Image Processing*, vol. 39, no. 3, pp. 355–368, 1987.
- [2] D. J. Jobson, Z. Rahman, and G. A. Woodell, “A multiscale Retinex for bridging the gap between color images and the human observation of scenes,” *IEEE Trans. Image Process.*, vol. 6, no. 7, pp. 965–976, 1997.
- [3] D. J. Jobson, Z. Rahman, and G. A. Woodell, “Properties and performance of a center/surround Retinex,” *IEEE Trans. Image Process.*, vol. 6, no. 3, pp. 451–462, 1997.
- [4] Q. Wang and Y. Cai, “Naturalness-preserved enhancement algorithm for non-uniform illumination images,” *IEEE Trans. Image Process.*, vol. 22, no. 9, pp. 3538–3548, 2013.
- [5] X. Guo, Y. Li, and H. Ling, “LIME: Low-light image enhancement via illumination map estimation,” *IEEE Trans. Image Process.*, vol. 26, no. 2, pp. 982–993, 2017.
- [6] X. Fu *et al.*, “A weighted variational model for simultaneous reflectance and illumination estimation,” in *Proc. CVPR*, 2016, pp. 2782–2790.
- [7] D. Krishnan and R. Fergus, “Dark flash photography,” in *ACM SIGGRAPH*, 2009.
- [8] T. Matsui, M. Iwahashi, and H. Kiya, “Image deblurring using multiple differently exposed images with infrared flash,” in *IEEE ICIP*, 2009.
- [9] M. Awad, A. Elliethy, and H. A. Aly, “Adaptive near-infrared and visible fusion for fast image enhancement,” *IEEE Trans. Comput. Imaging*, vol. 6, pp. 408–421, 2020.
- [10] K. G. Lore, A. Akintayo, and S. Sarkar, “LLNet: A deep auto-encoder approach to natural low-light image enhancement,” *Pattern Recognition*, vol. 61, pp. 650–662, 2017.
- [11] C. Chen *et al.*, “Learning to see in the dark,” in *Proc. CVPR*, 2018, pp. 3291–3300.

-
- [12] Y. Jiang *et al.*, “EnlightenGAN: Deep light enhancement without paired supervision,” *arXiv:1906.06972*, 2019.
 - [13] Y. Zhang *et al.*, “Beyond brightening low-light images,” *IEEE Trans. Image Process.*, vol. 30, pp. 889–900, 2021.
 - [14] C. Guo *et al.*, “Zero-reference deep curve estimation for low-light image enhancement,” in *Proc. CVPR*, 2020, pp. 1780–1789.
 - [15] J. Chen *et al.*, “SwinIR: Image restoration using Swin Transformer,” in *Proc. ICCV*, 2021.
 - [16] Z. Fei, R. K. Ward, and X. Li, “Low-light image enhancement via diffusion models,” in *Proc. CVPR*, 2023.
 - [17] D. Ulyanov, A. Vedaldi, and V. Lempitsky, “Deep image prior,” in *Proc. CVPR*, 2018, pp. 9446–9454.
 - [18] T. Chobola *et al.*, “Fast context-based low-light image enhancement via neural implicit representations,” in *Proc. ECCV*, 2024.
 - [19] L. Ma, T. Ma, R. Liu, X. Fan, and Z. Luo, “Toward fast, flexible, and robust low-light image enhancement,” in *Proc. CVPR*, 2022, pp. 5637–5646.
 - [20] R. Liu, L. Ma, J. Zhang, X. Fan, and Z. Luo, “Retinex-inspired unrolling with cooperative prior architecture search for low-light image enhancement,” in *Proc. CVPR*, 2021, pp. 10561–10570.
 - [21] Z. Fu *et al.*, “Learning a simple low-light image enhancer from paired low-light instances,” in *Proc. CVPR*, 2023, pp. 22252–22262.
 - [22] J. Y. Zhu, T. Park, P. Isola, and A. A. Efros, “Unpaired image-to-image translation using cycle-consistent adversarial networks,” in *Proc. ICCV*, 2017, pp. 2223–2232.
 - [23] C. Xie, H. Tang, L. Fei, H. Zhu, and Y. Hu, “IRNet: An improved zero-shot Retinex network for low-light image enhancement,” *Electronics*, vol. 12, no. 14, Art. 3162, 2023.



Digital Receipt

This receipt acknowledges that Turnitin received your paper. Below you will find the receipt information regarding your submission.

The first page of your submissions is displayed below.

Submission author: Hirak Medhi
Assignment title: Quick Submit
Submission title: Thesis
File name: Hirak_Thesis.pdf
File size: 1.07M
Page count: 25
Word count: 6,278
Character count: 35,045
Submission date: 06-May-2025 12:43PM (UTC+0530)
Submission ID: 2667937167

Abstract

Photography and vision systems consistently fail when photon counts drop: shot noise takes over, colours fade out, and fine structure vanishes. Traditional low-light enhancement pipelines either (i) depend on supervised learning with limited paired data, (ii) hallucinate detail at the expense of heavy priors that smear textures, or (iii) are too computationally expensive on resource-limited devices. This thesis introduces a *zero-shot* enhancement pipeline that co-processes a dirty RGB exposure and its synchronised near-infrared (NIR) counterpart—captured by commodity “dark-flash” cameras—to recover faithful, noise-free images with no offline training.

The technique combines a per-image implicit lighting model, implemented with periodic SIREN layers, with a fast, edge-aware NIR fusion stage and a guided-filter denoiser. A well-balanced loss cocktail—exposure, spatial fidelity, total-variation smoothness, sparsity loss and NIR structured loss—optimises the lighting map on-the-fly. Qualitative examination and a controlled user test further verify enhanced colour constancy, edge acuity and noise elimination.

By dispelling the necessity for paired training data and heavy networks, the research makes low-light improvement feasible for mobile imaging, night-vision surveillance and field robotics, and points to broader potential in cross-modal, training-free restoration techniques.

Keywords: Low-light image enhancement, Near-infrared fusion, Zero-shot learning.

Thesis

ORIGINALITY REPORT

3%

SIMILARITY INDEX

4%

INTERNET SOURCES

4%

PUBLICATIONS

1%

STUDENT PAPERS

MATCH ALL SOURCES (ONLY SELECTED SOURCE PRINTED)

2%

★ arxiv.org

Internet Source

Exclude quotes On

Exclude bibliography On

Exclude matches < 14 words